Sensors and Actuators A 194 (2013) 269–276

Contents lists available at SciVerse ScienceDirect

Sensors and Actuators A: Physical

journal homepage: www.elsevier.com/locate/sna

A piezoelectric-driven rotary actuator by means of inchworm motion

Jianping Li[a], Hongwei Zhao[a,*], Han Qu[a], Tao Cui[a], Lu Fu[a], Hu Huang[a], Luquan Ren[b], Zunqiang Fan[a]

[a] College of Mechanical Science & Engineering, Jilin University, Changchun, 130025, China
[b] School for Biology and Agricultural Engineering, Jilin University, Changchun, 130025, China

ARTICLE INFO

Article history:
Received 6 November 2012
Received in revised form 10 February 2013
Accepted 13 February 2013
Available online 26 February 2013

Keywords:
Piezoelectric actuator
Inchworm
Flexure hinge
Rotary
Positioning system

ABSTRACT

This paper presents a piezoelectric-driven stepping rotary actuator based on the inchworm motion. With the help of nine piezoelectric stacks and the flexure hinges, the designed actuator can realize large rotary ranges and high rotary speed with high accuracy. Three kinds of working units that compose the actuator are described and calculated: the clamping unit to hold the rotor, the adjusting unit to preload the piezoelectric stacks and the driving unit to produce the driving torque. To test the working performance, a prototype actuator was fabricated, and the experimental results indicate that the minimum stepping angle is 4.95 μrad when the driving voltage is 20 V and the frequency is 1 Hz, the maximum output torque is 93.1 N mm under the driving voltage of 100 V and the maximum velocity can be 6508.5 μrad/s when the frequency reaches 30 Hz. The experimental results verify that the proposed actuator can realize different stepping angles and rotation speeds with high accuracy under different driving voltages and frequencies.

1. Introduction

With the development of science and technology, the precision positioning system is more and more important in the fields of precision and ultra-precision manufacture, nanotechnology, semiconductor, MEMS and so on. Up to now, many novel types of actuators have been developed and the piezoelectric-driven actuator is one of them [1]. Due to its advantages: small size, high resolution, rapid response and low energy consumption, the piezoelectric-driven actuator is suitable for the precise positioning system. So far, the piezoelectric-driven actuator can be mainly classified into ultrasonic actuators [2–5], Inertial stepping actuators [6–11], inchworm actuators [12–17] and so on. Ultrasonic actuators are based on elliptical motion realized by piezoelectric vibration bodies, and at the action of friction the actuators can reach high speed, but the output force and the high resolution motion are still the difficulties. Inertial stepping actuators are usually composed of only one active component, hence they are easy to control and have a high response speed. Inchworm actuators usually have large motion ranges and high output torques, thus much attention has been paid to them during these years.

But so far most of the inchworm actuators are linear actuators [12–16], only a few rotary actuations using inchworm principle are provided [17–20]. And some of them have limited ranges [19], others have difficulties on the output torques [17,18]. This paper presents a piezoelectric-driven rotary actuator based on the inchworm principle to achieve the rotary movement. With the help of nine piezoelectric stacks and flexure hinges, the designed actuator can realize stepping rotary movement with high accuracy. The flexure hinges are designed to realize the needed force and can also reduce the number of components and the assembly effort. The experimental results suggest that this actuator has a large motion range and high position accuracy. This novel actuator has some reference significance for the application of the inchworm principle and flexure hinges in the design of the piezoelectric-driven actuators.

2. Structure analysis

As shown in Fig. 1, the structure of a new piezoelectric-driven rotary actuator is given. To improve the elastic properties of the flexure hinges, the material of the stator is 65 Mn.

The stator includes two layers which are connected by flexure hinges. Moreover, there are three piezoelectric stacks in each layer to push three clamping units respectively, so that the rotor can be clamped or released at the right time. And the piezoelectric stacks are preloaded by the adjusting units using shim block structures. Assembled at the outboard side of the stator are three driving units, the three piezoelectric stacks in driving units will produce the torque together with the connecting flexure hinges between the upper layer and the under layer of the stator. To ensure the working precision, all the parts are assembled carefully.

* Corresponding author. Tel.: +86 431 85095428; fax: +86 431 85095428.
E-mail addresses: hwzhao@jlu.edu.cn, huanghu0691@mails.jlu.edu.cn (H. Zhao).

0924-4247/$ – see front matter © 2013 Elsevier B.V. All rights reserved.
http://dx.doi.org/10.1016/j.sna.2013.02.020

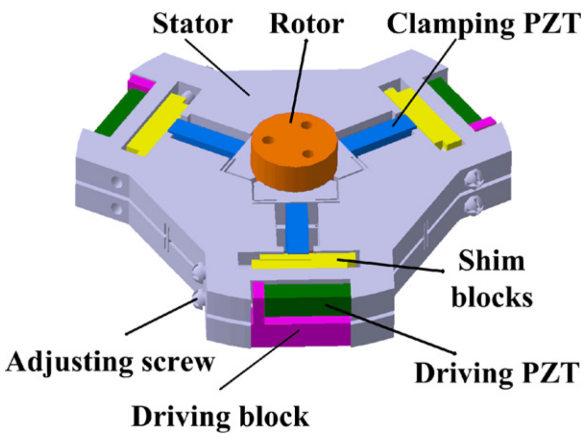

Fig. 1. Model of the designed rotary actuator.

According to the function, all the parts of the designed actuator can be divided into three kinds of units: the clamping unit, the adjusting unit and the driving unit.

2.1. The clamping unit

As shown in Fig. 2, to realize enough clamping force, the actuator uses three clamping units in each layer, so there are six clamping units in all. The clamping units are of great importance for that the performance of the actuator is based on whether the clamping units in each layer can hold the rotor tightly at the right time. When the clamping piezoelectric stacks get charged, they will expend to push the clamping flexure hinges. At the action of the flexure hinges, the clamps can hold the rotor tightly. The advantages of the structure that uses three clamping units placed 120° apart from each other are the large output force and the self-centering characteristic. Friction principle is used when the clamping units are working. Fig. 3 shows the force condition of the rotor when it rotates in the clockwise direction.

If the rotor is clamped tightly, the following equation must be satisfied and the output torque can also be got:

$$M = 3f_0R - M_0 - M_e \geq 0 \quad (1)$$

$$f_0 = \mu F \quad (2)$$

where M is the output torque of the actuator (N·m); f_0 is the friction force between the rotor and the clamp; μ is the friction coefficient between the rotor and the clamp; F is the force to hold the rotor

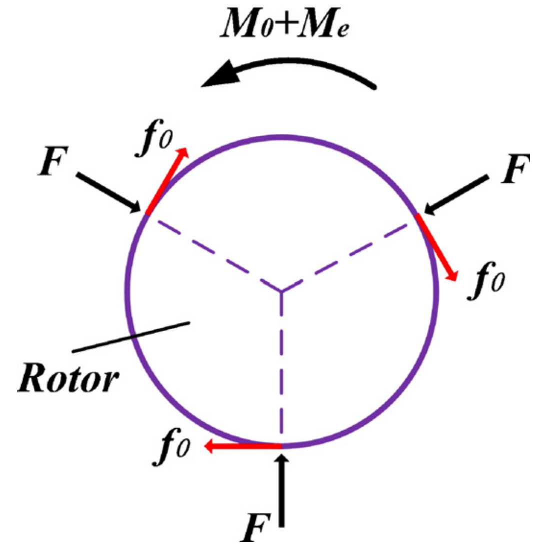

Fig. 3. The force condition of the rotor.

provided by each clamping unit (N); M_0 is the inertia moment of the rotor (N·m); M_e is the external load moment (N·m).

Fig. 4 provides the contact stress distribution between the clamping units and the rotor on the simulating working condition in order to check the condition of the stress distribution and whether the stress intensity is under the yield limit, which was taken through FEM (Finite Element Method). The materials of the stator and rotor are both 65 Mn fabricated by heat treatment and the friction coefficient between them is set as 0.1 during the analysis. Three piezoelectric stacks AE0505D08 from Tokin Company are used in the clamping units of each layer of the stator. When the driving voltage increases, the elongation of the piezoelectric stack becomes larger. If the driving voltage reaches 150 V, the largest elongation value of this piezoelectric stack is approximately 10 μm, hence the displacement loads of 10 μm were applied on the surfaces where the piezoelectric stacks are located. The result shows that the peak stress is on the place where the clamps and the rotor contact and the value is 411 Mpa which is under the yield limit of 784.27 MPa. According to the definition of the stress, the contact stress becomes larger when the clamping force increases for a given contact area. For this paper, the clamping force increases along with the displacement load which is controlled by the input voltage of the piezoelectric stack.

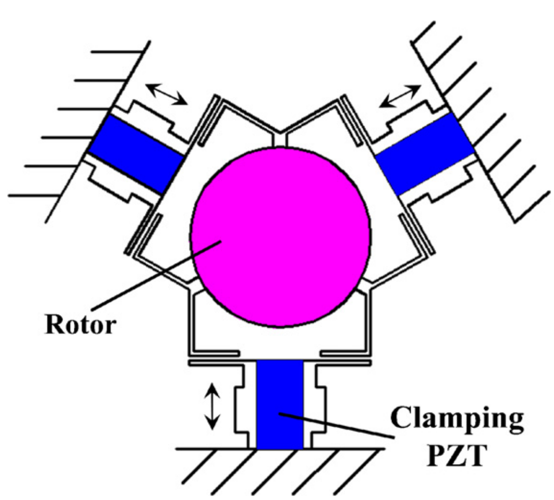

Fig. 2. Working schematic of the clamping unit.

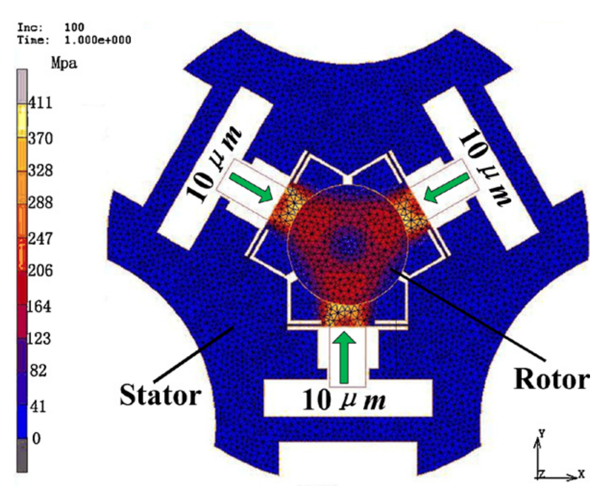

Fig. 4. Contact stress distribution of the clamping unit.